

Dual stimuli-responsive nanocarriers via a facile batch emulsion method for controlled release of Rose Bengal

*Original*

Dual stimuli-responsive nanocarriers via a facile batch emulsion method for controlled release of Rose Bengal / Egil, A. C.; Carmignani, A.; Battaglini, M.; Sengul, B. S.; Acar, E.; Ciofani, G.; Ozaydin Ince, G.. - In: JOURNAL OF DRUG DELIVERY SCIENCE AND TECHNOLOGY. - ISSN 1773-2247. - STAMPA. - 74:(2022), p. 103547. [10.1016/j.jddst.2022.103547]

*Availability:*

This version is available at: 11583/2970205 since: 2022-07-21T06:22:03Z

*Publisher:*

Elsevier

*Published*

DOI:10.1016/j.jddst.2022.103547

*Terms of use:*

This article is made available under terms and conditions as specified in the corresponding bibliographic description in the repository

*Publisher copyright*

(Article begins on next page)

# Dual Stimuli-Responsive Nanocarriers via a Facile Batch Emulsion Method for Controlled Release of Rose Bengal

Abdurrahim Can Egil<sup>a</sup>, Alessio Carmignani<sup>b</sup>, Matteo Battaglini<sup>b</sup>, Bengu Sueda Sengul<sup>a</sup>, Egemen Acar<sup>a</sup>, Gianni Ciofani<sup>b\*</sup>, Gozde Ozaydin Ince<sup>a,c,d \*</sup>

<sup>a</sup> Materials Science and Nano Engineering, Faculty of Engineering and Natural Sciences, Sabanci University, 34956, Istanbul, Turkey

<sup>b</sup> Smart Bio-Interfaces, Istituto Italiano di Tecnologia, Viale Rinaldo Piaggio 34, 56025 Pontedera, Italy

<sup>c</sup> Sabanci University Nanotechnology Research and Application Center (SUNUM), 34956, Istanbul, Turkey

<sup>d</sup>Center of Excellence for Functional Surfaces and Interfaces (EFSUN), Sabanci University, 34956, Istanbul, Turkey

## Abstract

Stimuli-responsive nanocarriers (SRN) hold great potential as drug delivery systems due to the ability to tune the release of the drugs by controlling the external stimuli. However, the synthesis of SRNs with layers of different functional polymers within their structure generally requires tedious processing steps involving surfactants. In this work, we report the synthesis of dual-responsive SRNs via a facile batch emulsion method without the use of any surfactants. The core-shell structure, which is composed of pH-responsive chitosan- polyacrylic acid complex shell and a temperature-responsive poly (n-vinyl caprolactam) core, is designed to tune the release of a model drug, Rose Bengal (RB), by controlling the pH and the temperature of the medium. At high pH values, fast release of the RB is observed within the first 24 h with release amounts in the range of 55 - 90 %, depending on the temperature. At low pH values, on the other hand, sustained release of RB is observed with release amounts of approximately 10% within the first 24 h. Increasing the temperature from 25°C to 40°C increases the release rates and the total amount of RB released, confirming the temperature-dependent release kinetics of the SRNs. *In vitro* studies performed on human colorectal adenocarcinoma cells show that encapsulation of RB inside the SRNs promotes drug uptake by the cells, thus favoring a cytotoxic effect not observed in presence of the free drug.

Keywords: Nanoparticles, Stimuli-responsive drug delivery, Nanomedicine, Controlled release, Colon cancer

## 1. Introduction

Drug administration *via* the oral route is a highly preferred drug delivery method due to its simple and non-invasive nature. However, the digestive enzymes that are present in the gastrointestinal (GI) tract or the highly acidic environment of the stomach may lead to premature degradation or denaturation of the drug [1]. The variations in the pH of the gastrointestinal (GI) tract (from acidic in the stomach to slightly basic in the small intestine) or the temperature variations around the target tissue pose additional challenges when designing drug delivery systems (DDS) for colonic diseases with drug-specific release kinetics [2].

Stimuli-responsive nanocarriers (SRN), which release the drug at the target site, are promising solutions to the challenges faced during oral drug delivery. SRNs with pH and temperature control are recently gaining attention as drug delivery systems that facilitate drug release at high concentrations and sustained release rates at alkaline pH and high-temperature conditions of the colon environment [3], [4]. In one study involving SRNS, Kang *et al.* copolymerized N-Isopropylacrylamide (NIPAM) with N-vinylimidazole, to achieve pH and temperature-responsive release of a model protein, bovine serum albumin (BSA), and reported temperature and pH-dependent BSA release with approximately 35% of the BSA being released during the first 4 h [5]. On the other hand, Kim *et al.* reported the synthesis of copolymeric nanocarriers obtained from N-isopropyl acrylamide (NIPAM) and acrylic acid (AA) polymers *via* emulsion polymerization [6]. These dual responsive nanocarriers allowed the control of drug release rates by tuning the temperature and pH, leading to a difference of ~10% in the release amounts between the alkaline and acidic pH conditions. Jin *et al.* also used the same method to copolymerize NIPAM and AA and investigated the release kinetics of ibuprofen under different conditions. By tuning the polymer composition, they achieved a difference of 50% in the drug release amount at acidic and alkaline pH levels [7]. Chung *et al.* performed *in situ* surfactant-free polymerization of NIPAM in chitosan (CS)-poly (acrylic acid) (PAA) micelles and prepared dual responsive nanoparticles with 29% encapsulation efficiency of doxycycline hyclate. The dual responsive SRNs they synthesized showed a considerable difference between the drug release rates at alkaline and acidic pH levels. They obtained about 41% of drug release at the end of 14 days at alkaline pH level, whereas only about 23% of drug was released at acidic pH level [8].

Although many researches are available employing PNIPAM as a temperature-responsive polymer, recent studies on the cytotoxicity of PNIPAM due to its degradation into small amide derivatives in the acidic environment raise concerns about its use in nanomedicine, especially in oral drug delivery applications [9]. For this reason, the interest in another temperature-responsive polymer, poly(n-vinyl-caprolactam) (PNVCL), as more biocompatible alternative to PNIPAM in DDS, has recently increased significantly, especially for oral administration where nanoparticles are exposed to highly acidic conditions [10]. Fallon *et al.* reported the preparation of biocompatible pH/temperature-responsive

poly(N-vinylcaprolactam-co-itaconic acid) hydrogels by UV polymerization for the oral delivery of acetaminophen [11].

In another study, Mundargi *et al.*, prepared poly(N-vinylcaprolactam-co-methacrylic acid) microparticles by free radical polymerization for the oral administration of insulin, and demonstrated pH-responsive release of insulin from the microparticles with an encapsulation efficiency of 52% [12]. Medeiros *et al.*, on the other hand, prepared PNVCL and poly (NVCL-co-AA) microparticles using the spray drying method for the oral delivery of ketoprofen and reported pH-triggered release, where 42.6% of ketoprofen was released at the end of 10 days at alkaline pH, whereas this amount was only 11.5% at acidic pH [13]. Rao *et al.* copolymerized NVCL with acrylamidoglycolic acid (AGA) *via* surfactant-assisted batch emulsion polymerization method, to synthesize nanocarriers for the delivery of 5-fluorouracil at gastric and intestinal pH levels and temperatures [14]. They reported release rates of ~60% at pH of 1.2 and ~80% at pH of 7.4 at the end of 12 h, with encapsulation efficiencies < 62%.

Although dual responsive SRNs hold potential as drug delivery systems, use of surfactants, multi-step synthesis processes, and low encapsulation efficiencies impede their widespread use. In this study, we demonstrate the synthesis of dual responsive nanocarriers based on a core-shell structure *via* a simple batch emulsion method without the use of any surfactant. The synthesized nanocarriers have a chitosan polyacrylic acid polyelectrolyte complex shell and a poly (n-vinyl caprolactam) core and contain RB as a model drug. Following the fabrication of nanoparticles, characterization studies including size and zeta potential measurements by DLS, morphology analysis by SEM, and chemical characterization by FTIR are performed. Encapsulation efficiency and loading capacity of the nanoparticles and the release profiles at different pH levels and temperatures are determined. Finally, the therapeutic potential of the nanoparticles is investigated on Caco-2 cells in terms of cellular viability and internalization.

## 2. Experimental

### 2.1 Materials

Chitosan (75–85% deacetylated, low molecular weight, CAS no. 9012-76-4), Acrylic Acid (CAS Number: 79-10-7), N- vinyl-caprolactam (CAS Number 2235-00-9), N, N'-Methylenabisacrylamide (CAS Number 110-26-9), and Rose Bengal (CAS Number 632-69-9) were purchased from Sigma-Aldrich, USA. Acetic acid (CAS no. 64-19-7) was purchased from Merck, USA. Caco-2 cells (HTB-37™) were purchased from ATCC. Eagle's Minimum Essential Medium (EMEM), heat-inactivated fetal bovine serum (FBS, CAS Number 64742-49-0), penicillin-streptomycin (CAS Number 8025-06-7) were purchased from Gibco. Quant-iT™ PicoGreen® dsDNA Assay Kit and Hoechst were purchased from Invitrogen. WST-1 reagent (CAS Number 150849-52-8) was purchased from Roche. DiO (Vybrant™ Multicolor Cell-Labeling Kit, CAS Number 34215-57-1) was purchased from Thermo Fisher Scientific.

Paraformaldehyde (PFA, CAS Number 30525-89-4) and Phalloidin-Atto 488 were purchased from Sigma-Aldrich.

## **2.2 Preparation of Multiresponsive Nanoparticles**

Surfactant free batch emulsion polymerization technique was used in the synthesis of the CS/PAA/PNVCL nanoparticles. A proper amount of n-vinyl caprolactam (0.11 g) was dissolved in 20ml ultrapure double distilled water. After complete dissolution, 0.11 g acrylic acid and 0.25g chitosan were added to this solution. Sodium bicarbonate buffer (0.065 g) was used to maintain a constant pH value of the reaction mixture preventing hydrolysis of n-vinyl-caprolactam under acidic conditions.[15] The reaction mixture was placed in a reflux system and purged with nitrogen for 30 minutes. The temperature was adjusted to 80°C after purging and KPS solution (0.041 g in 5 ml) was injected to the system as the initiator for surfactant-free polymerization of n-vinyl-caprolactam (NVCL) and acrylic acid (AA) in the presence of chitosan. The solution became milky after 10 minutes of initiation. Polymerization was carried for 5 h, and the resulting solution was filtered (0.45 µm) then centrifugated at 40.000 rpm, 4°C for 45 min.

## **2.3 Preparation of Rose Bengal (RB) Loaded Multiresponsive Nanoparticles**

A diffusion-based drug loading technique was used to obtain drug-loaded nanoparticles. Briefly, a stock solution of blank nanoparticles was diluted 10 times and incubated in aqueous RB solution (0.25 mg/ml) for 72h at room temperature then centrifugated for 45 min at 40000 rpm and 4°C in order to remove the free RB molecules and calculate the encapsulation efficiency through the supernatant.

## **2.4 Characterization of the Multiresponsive Nanoparticles**

Hydrodynamic size, dispersity, and zeta potential values were measured using ZetaSizer Nano ZS (Malvern Instruments, UK) instrument, which contains a 4.0 mV Helium-Neon laser (633 nm). Size analyses were performed between 25°C to 45°C and at pH levels ranging from 3.5 to 6.5.

Chemical characterization of the particles was performed using Fourier-Transform Infrared Spectroscopy (Thermo Scientific, Nicolet, iS10, USA). UV-Vis spectroscopy was utilized in order to evaluate the encapsulation efficiency and the loading capacity of the nanoparticles and to determine the release profiles at different pH levels and temperatures.

The size and morphology of the synthesized nanoparticles were additionally assessed by a field-emission scanning electron microscope (Zeiss Leo Supra 35VP SEM-FEG, Germany) at a 3 kV operating voltage. 10ul of the nanoparticles were pipetted on a piece of the silicon wafer and dried for 5 h at room temperature. The dried samples were coated with Au-Pd using a sputter coater (Cressington 108, UK) at 40 mA for 120 s. The SEM images were obtained by the secondary electron (SE) detector. On the

other hand, 3  $\mu$ l of stock solution was pipetted on a transmission electron microscopy (TEM) grid, and analysis was performed at 200 kV using the device (JEMARM200, JEOL, Japan).

## 2.5 Drug Release Studies of the Multiresponsive Nanoparticles

For the release studies, RB-loaded nanoparticles were placed in dialysis capsules with a cellulose membrane of 12-14 kDa. The capsules were placed in beakers containing 50 ml of PBS at pH=3.0, 5.0 and 7.4 and incubated in shaking incubators at 25°C and 40°C. The pH values were varied within the range of 3 - 7.4 which are close to the pH variations in the gastrointestinal tracts to study the stability and response of the nanoparticles at these pH values. Temperature values, on the other hand, were chosen as 25 and 40°C to observe the temperature response of pNVCL which has the LCST temperature at 32°C.

The measurements were taken periodically over a time span of 120 h. 1 ml of release medium was removed from the beakers and RB concentration was determined via UV-Vis analysis. The percent drug release was then calculated using Eq. (1).

$$\text{Release}(\%) = \frac{\text{Released Amount of Drug}}{\text{Total Amount of Drug}} \times 100 \quad (1)$$

## 2.6 Cell culture

Caco-2 cells (ATCC® HTB-37™) were cultured in proliferation condition using Eagle's Minimum Essential Medium (EMEM, Gibco) supplemented with 20% heat-inactivated fetal bovine serum (FBS, Gibco) and 1% penicillin-streptomycin (100 IU/ml of penicillin and 100  $\mu$ g/ml of streptomycin, Gibco), at 37°C in an atmosphere of 5% CO<sub>2</sub>.

## 2.7 Cellular viability

Cellular viability was assessed using either the Quant-iT™ PicoGreen® dsDNA Assay Kit (Invitrogen) and the WST-1 assay (Roche). For both experiments, Caco-2 cells were seeded at 10000 cells/cm<sup>2</sup> density in a 96-well plate (Corning) and let adhere for 24 h. Cells were treated with increasing concentrations of free RB (0.00, 0.85, 1.70, 3.40, 8.50 and 17.00  $\mu$ g/ml), CS/PAA/PNVCL nanoparticles (0, 25, 50, 100, 250 and 500  $\mu$ g/ml), and RB-loaded CS/PAA/PNVCL nanoparticles (0, 25, 50, 100, 250 and 500  $\mu$ g/ml respectively corresponding to 0.00, 0.85, 1.70, 3.40, 8.50 and 17.00  $\mu$ g/ml of RB) and incubated for 24 and 72 h. After the treatment, cells were washed in Dulbecco's phosphate buffered saline (DPBS). Regarding the Quant-iT™ PicoGreen® dsDNA Assay, cells were suspended in 100  $\mu$ l of Milli-Q water, then subjected to four cycles of freeze/thaw (from -80°C to 37°C), to allow cellular lysis and dsDNA release. Quant-iT™ PicoGreen® dsDNA assay was carried out by mixing PicoGreen® reagent, buffer, and cell lysate in Corning Costar® 96-well black polystyrene plates following the

manufacturer's instructions. Fluorescence was measured with a Victor X3 Multilabel Plate Reader ( $\lambda_{\text{ex}}$  485 nm,  $\lambda_{\text{em}}$  535 nm). WST-1 assay was carried out by suspending the cells with 300  $\mu$ l of phenol red-free complete medium added with the WST-1 reagent (1:20 dilution), then 30 min of incubation at 37°C. Finally, absorbance at 450 nm was measured, again using a Victor X3 Multilabel Plate Reader. Values were expressed in % with respect to untreated controls.

## 2.8 Cellular internalization

DiO-stained CS/PAA/PNVCL Nanoparticles were prepared: 10  $\mu$ M of DiO (Vybrant™ Multicolor Cell-Labeling Kit, Thermo Fisher Scientific) were added to 1 ml of Milli-Q water containing 5 mg/ml of nanoparticles, and then stirred for 2 h at room temperature. Finally, the mixture was washed four times with Milli-Q water through centrifugation at 16602 g.

Cellular internalization was evaluated both with flow cytometry and with confocal microscopy imaging. For flow cytometry purposes, Caco-2 cells were seeded at 10000 cells/cm<sup>2</sup> density in a 24-well plate (Corning) and let adhere for 24 h. Therefore, cells were treated with 100  $\mu$ g/ml of DiO-stained CS/PAA/PNVCL nanoparticles and incubated for 24, 48, or 72 h. Finally, cells were washed in DPBS, detached from the wells, then analyzed with a CytoFLEX platform (Beckman Coulter,  $\lambda_{\text{ex}}$  488 nm, FITC  $\lambda_{\text{em}}$  525/40 nm). Regarding confocal microscopy experiments, Caco-2 cells were seeded at 10000 cells/cm<sup>2</sup> density in WillCo-dish® and let adhere for 24 h. Then, cells were treated with 100  $\mu$ g/ml of DiO-stained CS/PAA/PNVCL nanoparticles and incubated for 24, 48, or 72 h. After the incubation cells, were washed in DPBS, fixed with 4% paraformaldehyde (PFA, Sigma-Aldrich in DPBS) at 4°C for 20 min, and washed twice with DPBS. Cytoskeleton and nuclei of fixed cells were stained respectively with 2.5  $\mu$ g/ml of TRITC-phalloidin (Sigma) and 5  $\mu$ g/mL of Hoechst (Invitrogen), following standard staining protocols. Confocal microscopy images were acquired with a C2s system (Nikon) with a 60 $\times$  oil immersion objective.

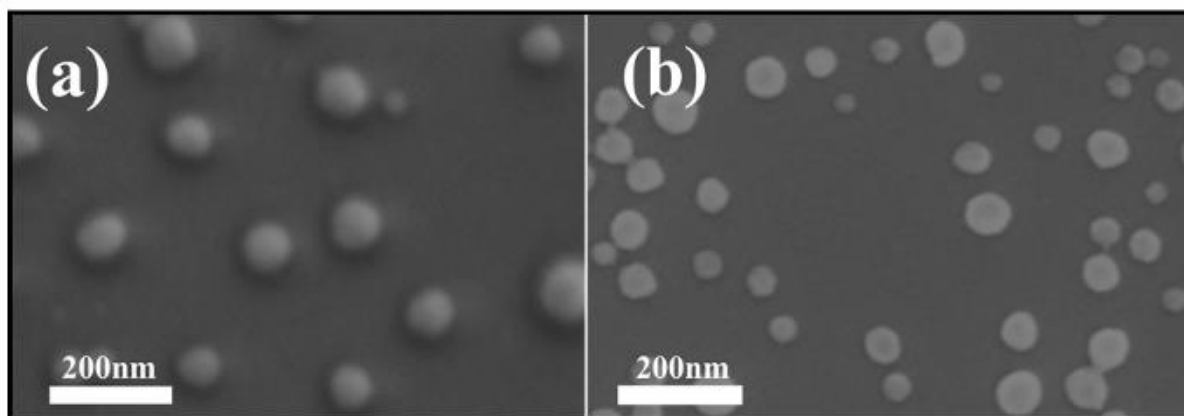
## 2.9 Statistical analysis

The normality of data distributions was verified with the Shapiro-Wilk normality test. Normally distributed data were analyzed *via* ANOVA, other data *via* Kruskal-Wallis followed by Wilcoxon signed-rank test. Each experiment has been performed in triplicate ( $n=3$ ), if not differently indicated.

# 3. Results and Discussion

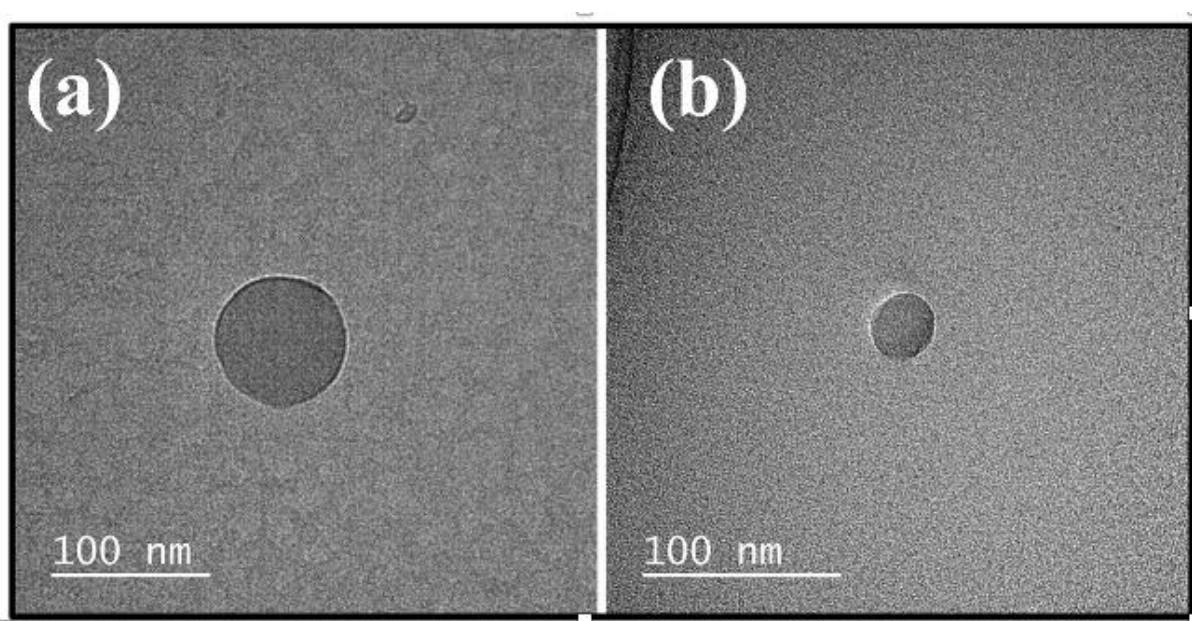
## 3.1 Characterization of Multiresponsive Nanoparticles

Figure 1 shows the SEM images of the blank (a) and drug-loaded (b) nanoparticles. For both blank and loaded nanoparticles, the average diameters were below 100 nm with uniform size distribution. Furthermore, comparing the SEM images it was observed that diffusion-based loading of the RB did not have a significant impact on the size and uniformity of the nanoparticles.



**Fig. 1.** SEM images of (a) blank and (b) loaded nanoparticles

For further analysis of the nanoparticle shape and structure, TEM analyses were performed. Figure 2 shows the TEM images of the (a) blank and (b) loaded nanoparticles. The TEM images confirmed the size and shape of the nanoparticles determined by the SEM analyses. In addition, the dark, outer shell observed in TEM images can be attributed to the chitosan-polyacrylic acid polyelectrolyte complex.



**Fig. 2.** TEM Images of Blank (a) and Loaded(b) Nanoparticles



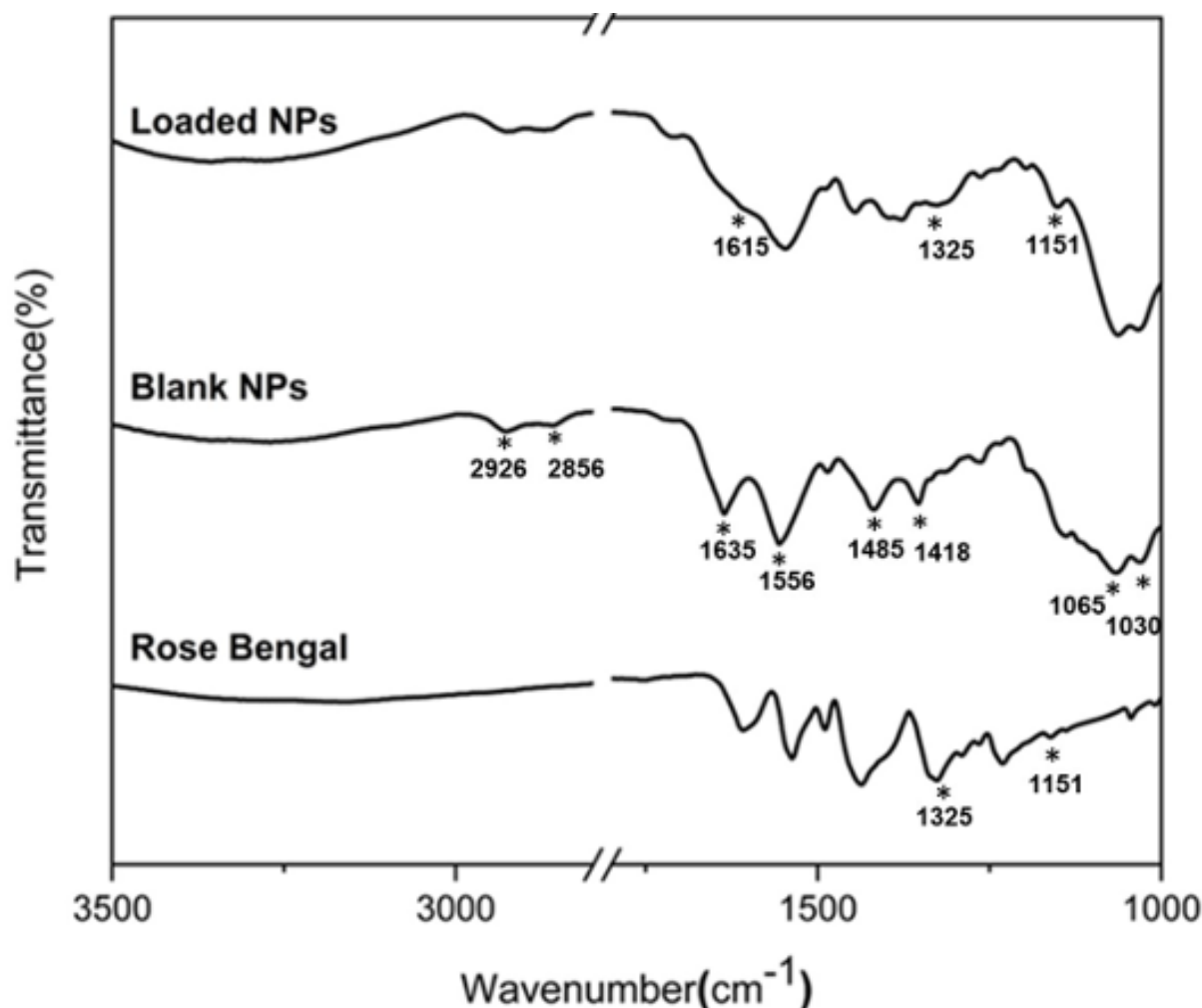


**Fig. 3.** FTIR Spectra of RB, Blank Nanoparticles, and RB Loaded Nanoparticles

FTIR analyses were performed for the chemical characterization of the nanoparticles. The spectra of blank nanoparticles, pure RB, and RB-loaded nanoparticles are shown in Figure 3. In the spectrum of blank nanoparticles, the presence of chitosan was confirmed through the peaks at  $1635\text{ cm}^{-1}$ ,  $1065\text{ cm}^{-1}$ , and  $1030\text{ cm}^{-1}$  which correspond to the amino group, C3-OH, and C6-OH respectively. The carboxylic acid compounds of the polyacrylic acid in the structure were detected at  $1556\text{ cm}^{-1}$  and  $1418\text{ cm}^{-1}$ . The characteristic peaks corresponding to the aliphatic CH stretching of PNVCL appear at  $2926\text{ cm}^{-1}$  and  $2856\text{ cm}^{-1}$ , also the peak at  $1485\text{ cm}^{-1}$  corresponds to the C-N stretching in the ring [15]. Formation of polyelectrolyte complex between the positively charged chitosan and negatively charged polyacrylic acid moieties was confirmed through the  $\text{NH}_3^+$  absorption of chitosan at  $1635\text{ cm}^{-1}$  and the symmetric and asymmetric  $\text{COO}^-$  absorption of polyacrylic acid at  $1556\text{ cm}^{-1}$  and  $1418\text{ cm}^{-1}$ , respectively. The FTIR analyses confirm that the carboxylic acid groups of polyacrylic acid are deprotonated during polymerization, turning into the anionic  $\text{COO}^-$  groups which then interact with the protonated groups of chitosan [16], [17]. The FTIR spectra of the loaded nanoparticles show the RB characteristic peaks at  $1325\text{ cm}^{-1}$  and  $1151\text{ cm}^{-1}$ , which correspond to the C=C stretching and C-H bending of RB, respectively.

In addition, the peak appearing at  $1615\text{ cm}^{-1}$  (C=O stretching) in the spectrum of the loaded nanoparticles confirms the presence of the RB [18].

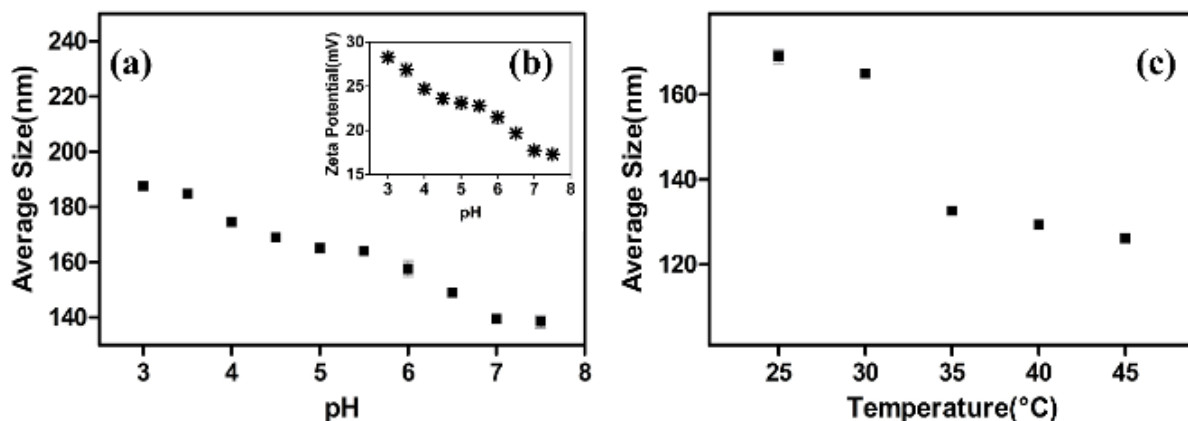


**Fig. 4.** (a) Average size and Zeta Potential Values of Blank nanoparticles at different pH levels at a constant temperature of 25°C, (b) zeta potential of Blank nanoparticles at different pH levels at a constant temperature of 25°C (c) average size of blank nanoparticles at different temperature levels (pH=4.5). Standard deviation values of the results of average size and zeta potential measurements are in the range of 0.32 to 0.81 for each data point

Figure 4 (a) shows that at 25°C, the average size of the nanoparticles decreases from  $187.7 \pm 1.2$  nm at pH=3.0 to  $138.5 \pm 2.3$  nm at pH=7.5. The zeta potential values also show a similar trend as pH increases. The change in size and zeta potential values with pH can be related to the changes in the ionization of chitosan ( $pK_a=6.0-6.5$ ) and polyacrylic acid ( $pK_a=4.25-4.5$ ) in the polyelectrolyte nanoparticle complex.

At the pH levels below 4.0, the amino groups of the chitosan are well protonated, resulting in the swelling of the chitosan shell which leads to the larger nanoparticle sizes measured. At pH levels between 4.0 and 6.0, the polyacrylic acid in the core is ionized, and the electrostatic interaction between the negatively charged carboxylic acid groups of the polyacrylic acid and positively charged amino groups of the chitosan results in a decrease in the nanoparticle size. As pH increases, chitosan chains start losing their charge and above pH 6.0, the chitosan chains collapse, leading to smaller nanoparticle sizes. These changes in ionization degrees of the pH-responsive polymers are also confirmed by the zeta potential values of the nanoparticles at different pH levels. The nanoparticles have  $28.3 \pm 0.6$  mV zeta potential at pH 3.0 whereas the zeta potential of the nanoparticles is  $17.3 \pm 0.6$  mV at pH 7.5. The decrease in the zeta potential of the nanoparticles can be attributed to both the ionization of the polyacrylic acid and the deprotonation of chitosan with increasing pH.

The temperature dependence of the nanoparticles is due to the presence of the temperature-responsive poly (n vinyl caprolactam) (pNVCL) in the core. At pH of 4.5, the average size of the nanoparticles decreases from  $169.0 \pm 1.7$  nm at 25°C to  $126.2 \pm 0.1$  nm at 45°C (Fig 4c), as a result of the collapsing of

the pNVCL chains at temperatures above LCST of 32°C. As seen in Fig 4c. around the LCST of 32°C, the sizes of the nanoparticles decrease from 165.0±0.1 nm at 30°C to 132.7±0.8 nm at 35°C.

Following the dynamic light scattering-based characterization studies of blank nanoparticles in terms of pH and temperature responsiveness, diffusion-based RB loading was done for 72 hours. During loading, the medium was maintained at a pH value of 4.5, where the chitosan chains are protonated through the NH<sub>3</sub><sup>+</sup> groups and can interact well with the COO<sup>-</sup> groups of RB. Furthermore, diffusion of RB molecules towards the core is facilitated at this pH where the polyacrylic acid chains are mostly neutral. Furthermore, the medium temperature was kept at room temperature during loading in order to operate below the LCST of pNVCL to improve the loading of the hydrophilic RB. After loading, the average size of the nanoparticles was measured as 163.0±0.9 nm with a 23.6±0.5 mV zeta potential value, indicating that the loading of the RB did not cause a significant increase in the nanoparticle size.

### 3.2 Drug Release Profile and Kinetic Analysis

Encapsulation efficiency of the RB-loaded nanoparticles is calculated as 93.66% ±1.55 using Eq. (2), where the amount of the free drug is determined from the UV-Vis measurements.

$$\text{Encapsulation Efficiency (\%)} = \frac{\text{Total Drug Amount} - \text{Free Drug Amount}}{\text{Total Drug Amount}} \times 100 \quad (2)$$

The loading capacity of the RB-loaded nanoparticles is calculated as 4.93% ±1.5 using Eq. 3, where the encapsulated drug amount is determined from Eq.2

$$\text{Loading Capacity (\%)} = \frac{\text{Encapsulated Drug Amount}}{\text{Total Nanoparticle Weight}} \times 100 \quad (3)$$

The results of the RB release studies from the loaded nanoparticles at different pH and temperature values are presented in Figure 5. At the acidic pH value of 3.0, only 2.19% and 1.77 % of RB was released at 25°C and 40°C, respectively, at the end of 120 hours. As the pH is increased from 5.0 to 7.4, the amount of RB released increases from 26% to 75.11% at 25°C and from 39.11% to 95.02% at 40°C, respectively. In addition to the cumulative drug release percentage, the pH of the medium also affected the release rates at the early stages. Comparing the release profiles at pH 5.0 and 7.4, at pH of 5.0, the drug release showed a linear behavior, indicative of a sustained release. On the other hand, at a higher pH value of 7.4, burst release of RB was observed, indicating the presence of a dominant pH-dependent mechanism. Considering the core-shell structure and the pH-dependent nature of the constituent polymers, the burst release observed at high pH is presumably due to the collapsing of the polymer chains which push the RB molecules out. Another factor is the electrostatic interaction between the pH-dependent moieties in the structure and the RB molecule. The nanoparticle structure is mainly a polyelectrolyte complex of negatively charged poly (acrylic acid) and positively charged chitosan chains. In acidic conditions, RB, which has a carboxylic acid group linked to one of its aromatic rings, can interact with the positively charged amino groups of chitosan. As pH increases, this interaction

becomes weaker as chitosan is deprotonated. On the other hand, formation of the negatively charged -COO<sup>-</sup> groups due to the deprotonation of the poly (acrylic acid) triggers the burst release of the RB molecules because of the electrostatic repulsion.

Under constant pH, increasing the temperature also increased total amount of RB released, though the effect of the temperature on the release kinetics was observed to be less significant than that of the pH. At the end of 120 h, 26% of RB was released at 25°C as opposed to 39.11% at 40°C at a constant pH of 5.0. Similarly, at pH of 7.4, 75.11% of RB was released at 25°C and 95.02% was released at 40°C. Temperature dependence was not observed at pH of 3.0, due to the negligible RB release at this low pH environment. The temperature dependence observed at pH 5.0 and 7.4 can be attributed to the conformational change in the pNVCL chains above LCST, leading to the transition from the hydrophilic to hydrophobic states. The increased hydrophobic nature of the polymer results in shrinking of the core structure which in turn, accelerates the drug release. This behavior is observed both at alkali and acidic pH levels. Ultimately, the consequence of the stimuli-responsive release of RB can be seen in the photograph of dialysis capsules after 72 h at 40°C, in the supplementary data.

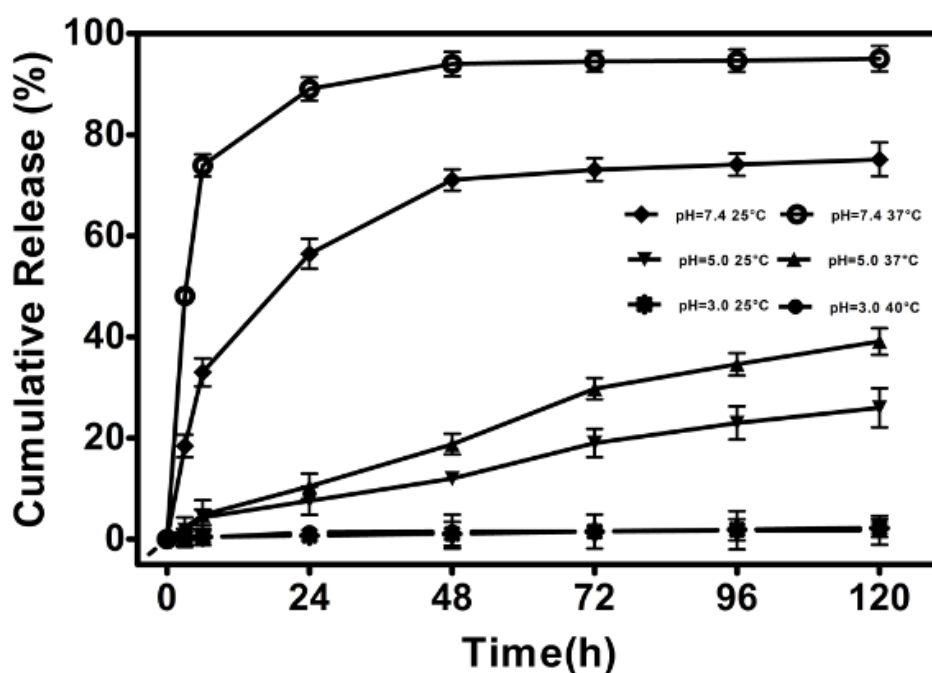


**Fig. 5.** Release Profiles of Nanoparticles in different temperature and pH levels. Standard deviation values of the release results are in the range of 0.14 to 0.55 for each data point

### 3.3 *In vitro* Studies

Dual responsive nanoparticles' interaction with cells was first analyzed by evaluating effects on Caco-2 cells viability. Cells were treated with increasing concentrations of free RB (0.00, 0.85, 1.70, 3.40, 8.50 and 17.00 µg/ml), blank nanoparticles (0, 25, 50, 100, 250 and 500 µg/ml), and RB-loaded nanoparticles (0, 25, 50, 100, 250 and 500 µg/ml respectively corresponding to 0.00, 0.85, 1.70, 3.40, 8.50 and 17.00

μg/ml of RB), and analyzed via both PicoGreen® and WST-1 assay, after 24 and 72 h of treatment. The results show that encapsulation of RB inside nanoparticles promotes a cytotoxic effect which is not observed with the free drug (Figure 6). Both analyses show a statistically significant ( $p < 0.001$ ) decrease in cell viability after 72 h of treatment with a concentration of RB-loaded nanoparticles of 100 μg/ml or more. In particular, PicoGreen assay results show a statistically significant ( $p < 0.001$ ) 52.2% decrement in viability after 72 h of treatment with the highest tested concentration of RB-loaded nanoparticles, compared to the cells treated with free RB.

In earlier studies reported by Qin *et al.* and by Koevary *et al.*, where the effectiveness of RB was tested on colon cancer cells with immunotherapeutic purposes and on various cell types, respectively, a statistically significant reduction ( $p < 0.001$ ) of cell viability is achieved with free RB concentrations of higher than 48 μg/ml [19][20]. In our work, we obtained comparable results with 14 times lower quantities of RB encapsulated within the nanoparticles. In particular, by comparing our results with those obtained on colon cancer cells in the work of Qin *et al.*, we obtained a statistically significant reduction ( $p < 0.001$ ) of cell viability using a 28 times lower quantity of RB loaded inside the nanoparticles. This significant reduction in cell viability, for the same amount of RB supplied, could be due to its encapsulation within the nanoparticles, which due to their lipophilic nature, could have increased the internalization of RB by treated cells.

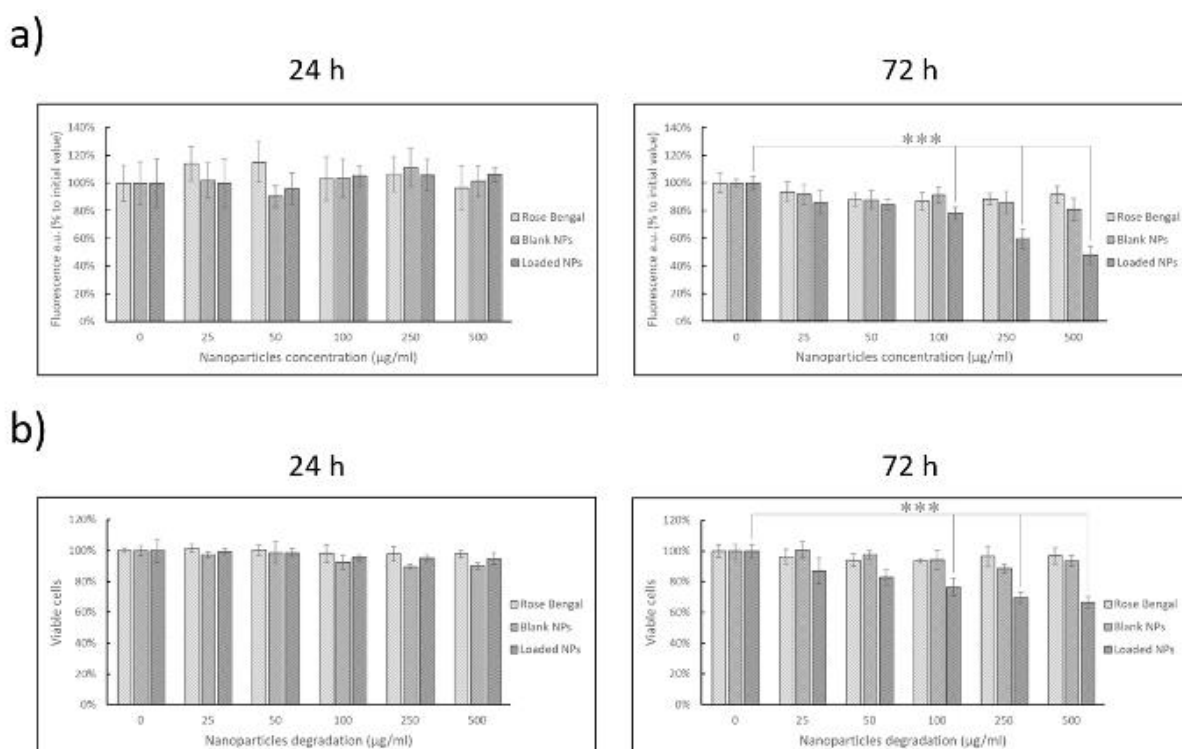
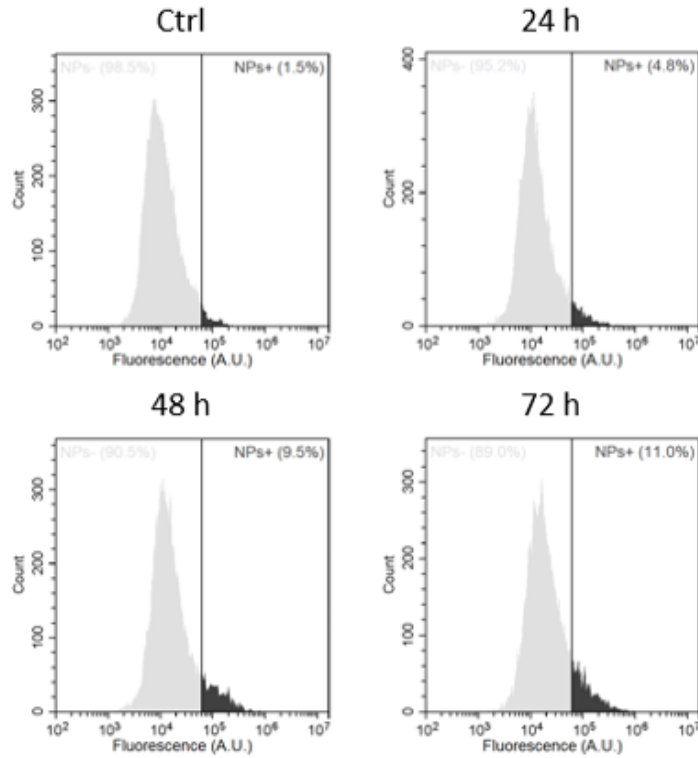


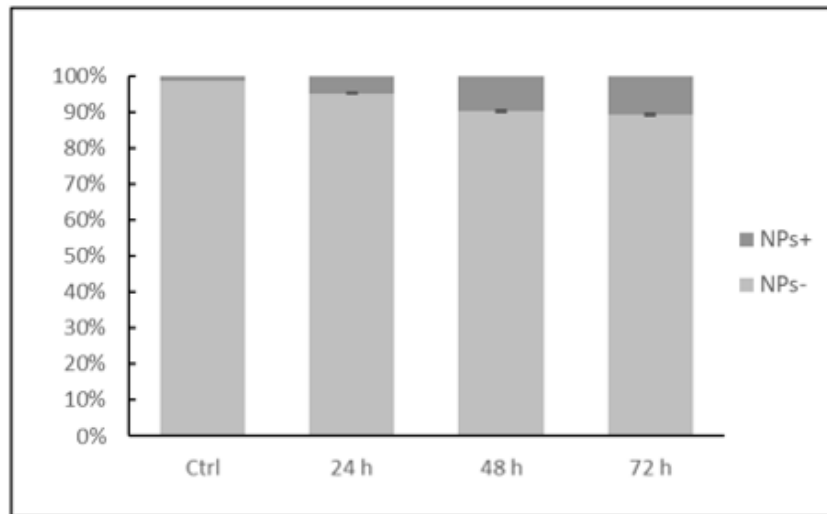
**Fig. 6.** Viability analysis on Caco-2 cells performed with increasing concentration of free RB, CS/PAA/PNVCL nanoparticles, and RB-loaded nanoparticles, at 24 h and 72 h. In a) results from PicoGreen assay, in b) results of WST-1 assay (\*\*\*)  $p < 0.001$  ( $n=6$ ).

To assess cellular internalization, fluorescently labeled CS/PAA/PNVCL nanoparticles were exploited. Cells were treated with 100  $\mu\text{g/ml}$  of nanoparticles for 24, 48, and 72 h, and then analyzed. Flow cytometry analysis showed  $4.8\% \pm 0.2\%$  of fluorescence-positive cells after 24 h, a result that increased up to  $11.0 \pm 0.8\%$  of fluorescence-positive cells after 72 h of treatment (Figure 7), showing a time-dependent internalization of these nanoparticles by Caco-2 cells. Confocal microscopy imaging confirms the trend observed via flow cytometry, highlighting a perinuclear localization of CS/PAA/PNVCL nanoparticles (Figure 8). Both techniques showed how the encapsulation of RB in these structures can overcome the cytosolic internalization problem of the administration of free RB in acetate form[21].

a)



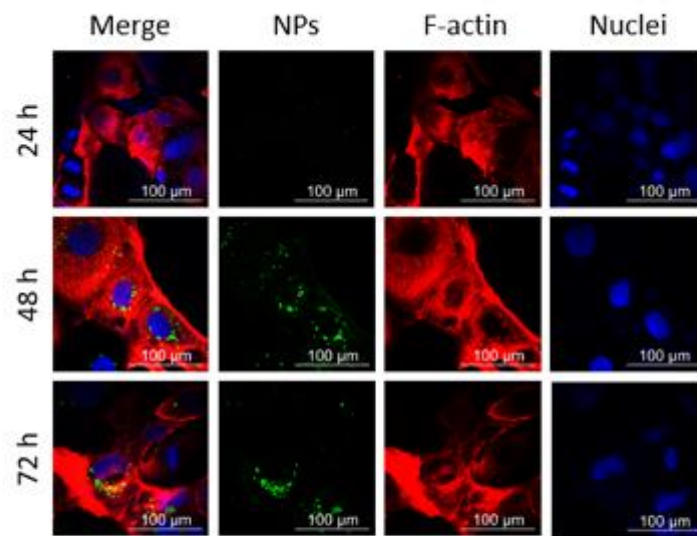
b)



336

337 **Fig. 7.** Flow cytometry analysis of Caco-2 cells incubated with 100  $\mu$ g/ml of DiO-stained nanoparticles  
 338 at different time points (24, 48, and 72 h). In dark grey nanoparticles-positive cells (NPs+), in light grey  
 339 nanoparticles-negative cells (NPs-). a) Representative flow cytometry plots showing fluorescence levels  
 340 of cells in different experimental conditions. (b) Percentages of NPs+ and NPs- cells for each  
 341 experimental condition ( $n=3$ ).

a)



b)

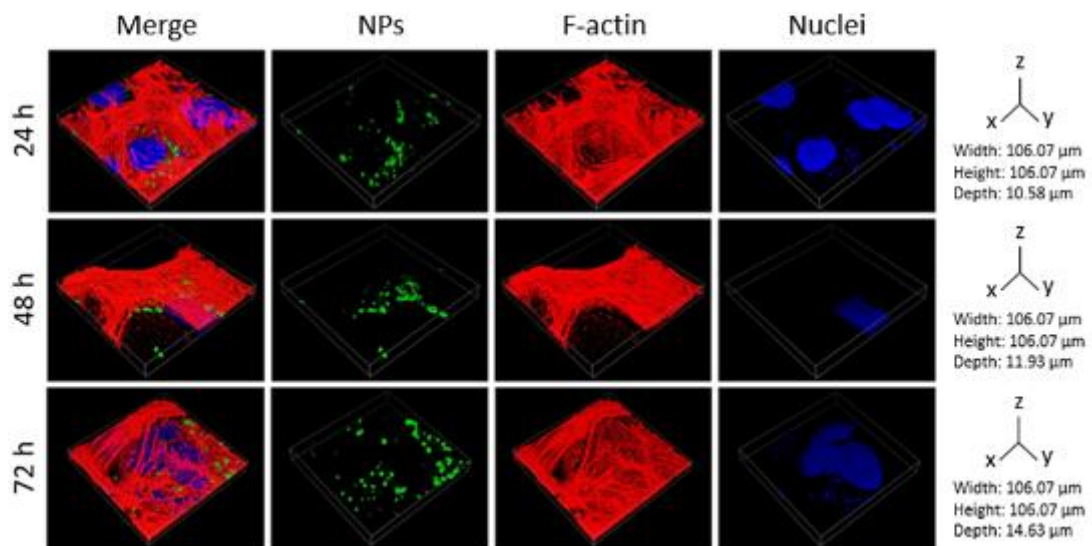


**Fig. 8.** Representative confocal images of Caco-2 cells incubated with 100 µg/ml of DiO-stained nanoparticles at different time points (24, 48, and 72 h, nanoparticles in green, F-actin in red, nuclei in blue): a) single Z-stacks and b) 3D rendering.



## 4. Conclusion

Stimuli-responsive nanocarriers (SRNs) composed of a pH-responsive chitosan / polyacrylic acid complex shell and a temperature-responsive poly (n-vinyl caprolactam) core, were synthesized *via* a facile batch emulsion method without the use of any surfactants. Fast release of the RB was achieved at pH 7.4, with more than 70% of the drug released within the first 10 h, whereas at pH 5.0 sustained release with a release percentage of approximately 10% was achieved at the end of 24 h. Furthermore, the therapeutic potential of RB-loaded SRNs against colon cancer cells (Caco-2 cell line) was investigated, and it was observed that RB-loaded nanoparticles displayed considerable cytotoxicity with respect to free RB, suggesting that the SRNs promote the cellular uptake of the RB. The pH and temperature-dependent release behavior of the nanocarriers, in addition to the improved drug uptake by the cells, make these SRNs promising candidates for the treatment of colon cancer *via* oral drug delivery.

## Credit Author Contribution Statement

**ACE:** Conceptualization, Methodology, Investigation, Formal analysis, Visualization, Writing – original draft. **AC:** Methodology, Investigation, Formal analysis, Visualization, Writing – original draft. **MB, EA, BSS:** Methodology, Formal analysis. **GC:** Supervision, Resources, Writing – review and editing. **GC, GOI:** Conceptualization, Supervision, Project administration, Resources, Validation, Writing – review and editing

## Acknowledgement

We would like to thank Prof. Mehmet Ali Gulgun for the TEM analysis. We would also like to thank Dr. Tugce Akkas for the UV-Vis analysis.

## Declaration of Competing Interest

All authors declare that they do not have any financial interests or personal relationships that could influence the work reported in this paper.

## REFERENCES

- [1] Choudhary, L., Jain, A., & Agarwal D. Colon-Targeted Oral Drug Delivery Systems: A Review. *Asian J Pharm Res Dev.* 2020;8(4):186-193. doi:10.22270/ajprd.v8i4.689
- [2] Amidon S, Brown JE, Dave VS. Colon-Targeted Oral Drug Delivery Systems: Design Trends and Approaches. *AAPS PharmSciTech.* 2015;16(4):731-741. doi:10.1208/s12249-015-0350-9
- [3] Tiwari A, Verma A, Panda PK, Saraf S, Jain A, Jain SK. Stimuli-Responsive Polysaccharides for Colon-Targeted Drug Delivery. Elsevier Ltd.; 2018. doi:10.1016/B978-0-08-101995-5.00022-2
- [4] Joseph SK, Sabitha M, Nair SC. Stimuli-responsive polymeric nanosystem for colon specific drug delivery. *Adv Pharm Bull.* 2020;10(1):1-12. doi:10.15171/apb.2020.001
- [5] Kang JH, Hwang JY, Seo JW, Kim HS, Shin US. Small intestine- and colon-specific smart oral drug delivery system with controlled release characteristic. *Mater Sci Eng C.* 2018;91(September 2017):247-254. doi: 10.1016/j.msec.2018.05.052
- [6] Kim YK, Kim EJ, Lim JH, et al. Dual Stimuli-Triggered Nanogels in Response to Temperature and pH Changes for Controlled Drug Release. *Nanoscale Res Lett.* 2019;14. doi:10.1186/s11671-019-2909-y
- [7] Jin X, Wang Q, Sun J, Panezail H, Wu X, Bai S. Dual temperature- and pH-responsive ibuprofen delivery from poly (N-isopropylacrylamide-co-acrylic acid) nanoparticles and their fractal features. *Polym Bull.* 2017;74(9):3619-3638. doi:10.1007/s00289-017-1915-4
- [8] Chung-Yang Chuang, Trong-Ming Don W-YC. Synthesis and Properties of Chitosan-Based Thermo- and pH-Responsive Nanoparticles and Application in Drug Release. *J Polym Sci Part A Polym Chem Vol 47.* 2009; 47:2798–2810. doi:10.1002/pola
- [9] Ramos J, Imaz A, Forcada J. Temperature-sensitive nanogels: poly(N-vinylcaprolactam) versus poly(N-isopropylacrylamide). *Polym Chem.* 2012;3(4):852-856. doi:10.1039/C2PY00485B
- [10] Cortez-Lemus NA, Licea-Claverie A. Poly(N-vinylcaprolactam), a comprehensive review on a thermoresponsive polymer becoming popular. *Prog Polym Sci.* 2016; 53:1-51. doi: 10.1016/j.progpolymsci.2015.08.001
- [11] Fallon M, Halligan S, Pezzoli R, Geever L, Higginbotham C. Synthesis and Characterisation of Novel Temperature and pH Sensitive Physically Cross-Linked Poly(N-vinylcaprolactam-co-itaconic Acid) Hydrogels for Drug Delivery. *Gels.* 2019;5(3). doi:10.3390/gels5030041
- [12] Mundargi RC, Rangaswamy V, Aminabhavi TM. Poly (N-vinylcaprolactam-co-methacrylic acid) hydrogel microparticles for oral insulin delivery. *J Microencapsul.* 2011;28(5):384-394. doi:10.3109/02652048.2011.576782
- [13] Medeiros SF, Lopes M V., Rossi-Bergmann B, Ré MI, Santos AM. Synthesis and characterization of poly(N-vinylcaprolactam)-based spray-dried microparticles exhibiting temperature and pH-sensitive properties for controlled release of ketoprofen. *Drug Dev Ind Pharm.* 2017;43(9):1519-1529. doi:10.1080/03639045.2017.1321660
- [14] Madhusudana Rao K, Mallikarjuna B, Krishna Rao KS V, Siraj S, Chowdoji Rao K, Subha MCS. Novel thermo/pH sensitive nanogels composed from poly(N-vinylcaprolactam) for controlled release of an anticancer drug. *Colloids Surfaces B Biointerfaces.* 2013; 102:891-897. doi: https://doi.org/10.1016/j.colsurfb.2012.09.009
- [15] Kozanoğlu S, Özdemir T, Usanmaz A. Polymerization of N-Vinylcaprolactam and Characterization of Poly(N-Vinylcaprolactam). *J Macromol Sci Part A.* 2011;48(6):467-477. doi:10.1080/10601325.2011.573350

- [16] Hu Y, Jiang X, Ding Y, Ge H, Yuan Y, Yang C. Synthesis and characterization of chitosan–poly (acrylic acid) nanoparticles. *Biomaterials*. 2002;23(15):3193-3201. doi: [https://doi.org/10.1016/S0142-9612\(02\)00071-6](https://doi.org/10.1016/S0142-9612(02)00071-6)
- [17] Saberi J, Ansari M, Ebrahimi Hoseinzadeh B, Kordestani SS, Naghib SM. Chitosan-Polyacrylic Acid Hybrid Nanoparticles as Novel Tissue Adhesive: Synthesis and Characterization. *Fibers Polym*. 2018;19(12):2458-2464. doi:10.1007/s12221-018-8762-2
- [18] Zeyada HM, Youssif MI, El-Ghamaz NA, Aboderbala MEO. Spectral, structural, optical and dielectrical studies of UV irradiated Rose Bengal thin films prepared by spin coating technique. *Phys B Condens Matter*. 2017; 506:75-82. doi: <https://doi.org/10.1016/j.physb.2016.10.044>
- [19] Qin J, Kunda N, Qiao G, et al. Colon cancer cell treatment with rose bengal generates a protective immune response via immunogenic cell death. *Cell Death Dis*. 2017;8(2): e2584. doi:10.1038/cddis.2016.473
- [20] Koevary SB. Selective toxicity of rose bengal to ovarian cancer cells in vitro. *Int J Physiol Pathophysiol Pharmacol*. 2012;4(2):99-107.
- [21] Manoil, D., Lange, N., & Bouillaguet, S. (2018). Enzyme-mediated photoinactivation of *Enterococcus faecalis* using Rose Bengal-acetate. *Journal of photochemistry and photobiology. B, Biology*, 179, 84–90. <https://doi.org/10.1016/j.jphotobiol.2018.01.001>

**APPENDIX A. SUPPLEMENTARY MATERIAL**

**Dual Stimuli-Responsive Nanocarriers via a Facile Batch Emulsion Method for Controlled Release of Rose Bengal**

Abdurrahim Can Egil<sup>a</sup>, Alessio Carmignani<sup>b</sup>, Matteo Battaglini<sup>b</sup>, Bengu Sueda Sengul<sup>a</sup>, Egemen Acar<sup>a</sup>, Gianni Ciofani<sup>b\*</sup>, Gozde Ozaydin Ince<sup>a,c,d \*</sup>

*a Materials Science and Nano Engineering, Faculty of Engineering and Natural Sciences, Sabanci University, 34956, Istanbul, Turkey*

*b Smart Bio-Interfaces, Istituto Italiano di Tecnologia, Viale Rinaldo Piaggio 34, 56025 Pontedera, Italy*

*c Sabanci University Nanotechnology Research and Application Center (SUNUM), 34956, Istanbul, Turkey*

*d Center of Excellence for Functional Surfaces and Interfaces (EFSUN), Sabanci University, 34956, Istanbul, Turkey*

\*Corresponding authors: gozde.ince@sabanciuniv.edu, gianni.ciofani@iit.it

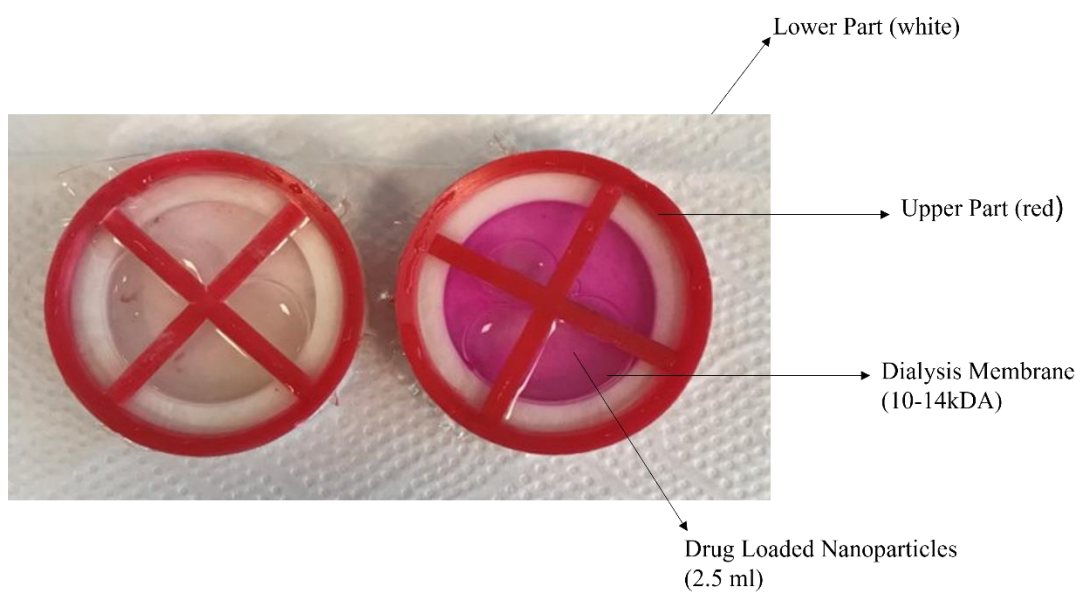


**Fig. S1.** The photograph of drug release capsules at pH=7.4(left) and pH=5.0 (right) after 72h at 40°C